

# Labile Cu(I) Catalyst/Spectator Cu(II) Species in Copper-Catalyzed C–C Coupling Reaction: Operando IR, in Situ XANES/EXAFS Evidence and Kinetic Investigations

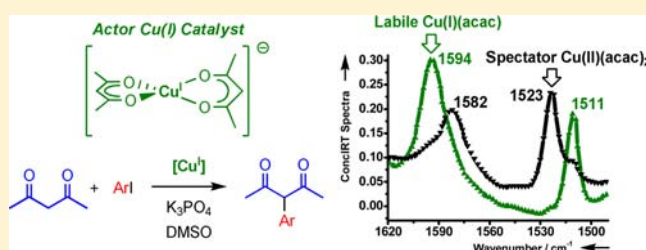
Chuan He,<sup>†</sup> Guanghui Zhang,<sup>†,‡</sup> Jie Ke,<sup>†</sup> Heng Zhang,<sup>†</sup> Jeffrey T. Miller,<sup>‡</sup> Arthur J. Kropf,<sup>‡</sup> and Aiwen Lei<sup>\*,†,‡</sup>

<sup>†</sup>College of Chemistry, Molecular Sciences, Wuhan University, Wuhan, 430072, People's Republic of China

<sup>‡</sup>Chemical Science, Engineering Division, Argonne National Laboratory, 9700 S. Cass Ave., Argonne, Illinois 60439, United States

**S** Supporting Information

**ABSTRACT:** Insights toward the Cu-catalyzed C–C coupling reaction were investigated through operando IR and in situ X-ray absorption near-edge structure/extended X-ray absorption fine structure. It was found that the Cu(I) complex formed from the reaction of CuI with  $\beta$ -diketone nucleophile was labile under the cross-coupling conditions, which is usually considered as active catalytic species. This labile Cu(I) complex could rapidly disproportionate to the spectator Cu(II) and Cu(0) species under the reaction conditions, which was an off-cycle process. In this copper-catalyzed C–C coupling reaction,  $\beta$ -diketone might act both as the substrate and the ligand.

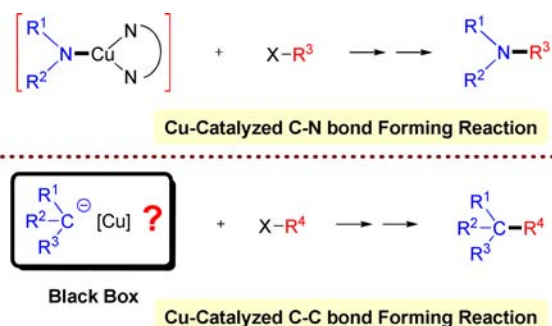


## INTRODUCTION

Since the pioneering and remarkable work reported by Ullmann and Goldberg in the last century, the copper-mediated C–C and C–heteroatom bond forming reactions have been well developed and extensively applied in academic and industrial areas.<sup>1</sup> However, there is still a general lack of knowledge about the mechanisms due to the easy accessibility of copper to multiple oxidation states and limited stability of compounds with C–Cu or N–Cu bonds.<sup>1a–c,f</sup> In these Cu-driven coupling processes, especially for C–heteroatom bond formations, the starting copper salts or copper complexes are usually used in various oxidation states including Cu(0), Cu(I), and Cu(II). It seems that almost any copper salt could be used as the precursor for the coupling reactions with similar behavior.<sup>1h,2</sup> Revealing the real active catalyst species must be the primary and fundamental task for the mechanistic investigations.

Early studies indicate that Cu(I) species might be the active catalyst in the copper-catalyzed C–heteroatom coupling reactions.<sup>2,3</sup> Recently, some insights toward copper-catalyzed arylation for C–N bond formation were discussed.<sup>3c–e,g,i,m,o</sup> Copper(I) amidate complexes of chelating 1,2-diamine ligands were proposed as the probable intermediates in the copper-catalyzed amidations (Scheme 1). Notably, Cu(0) precursor has been demonstrated to be oxidized by aryl halides to afford the active Cu(I) complex in the Ullmann-type reactions by using electrochemical techniques.<sup>3k</sup> Meanwhile, Cu(II) precursor could be reduced by alcohols or amines to generate active Cu(I) species in the reaction monitored by UV–vis and NMR spectroscopy.<sup>3j</sup> Besides the C–heteroatom couplings,

## Scheme 1. Active Copper Catalyst in C–N and C–C Coupling Reactions



copper-catalyzed arylation of C nucleophiles has also been used as one of the important C–C bond forming reactions.<sup>1c,d,t,4</sup> Some significant and efficient copper-catalyzed Hurtley-type arylations of  $\beta$ -dicarbonyl compounds have been reported in recent years.<sup>3h,5</sup> However, scarce examples were reported regarding the active catalyst and reaction mechanism (Scheme 1).<sup>6</sup> Herein, we communicate our direct observation of a complex formation between CuI and a  $\beta$ -diketone nucleophile monitored by operando IR and in situ X-ray absorption near-edge structure (XANES)/extended X-ray absorption fine structure (EXAFS).<sup>7</sup> We also identified that such a Cu(I) complex is very labile, which would rapidly disproportionate

Received: October 17, 2012

Published: December 7, 2012

into Cu(0) and Cu(acac)<sub>2</sub> as an off-cycle process in the reaction. Both experimental results and computational calculations indicated that the Cu(I)  $\beta$ -diketonate complex might be the active catalyst in the arylation reactions.

## RESULTS AND DISCUSSION

**Copper-Catalyzed C–C Bond Forming Reaction.** Due to the interest in the mechanism of copper-catalyzed C–C couplings, our initial effort was focused on the arylation of a C nucleophile using aryl iodides and  $\beta$ -diketones. In the early studies, we found that the direct arylation product was not easy to obtain under the typical conditions.<sup>5g</sup> Under anhydrous conditions, aryl iodide **1a** could react with acetylacetone **2a** affording the direct arylation product **3a**. The results are shown in Figure 1. Using 10 mol % CuI as the catalyst precursor, the

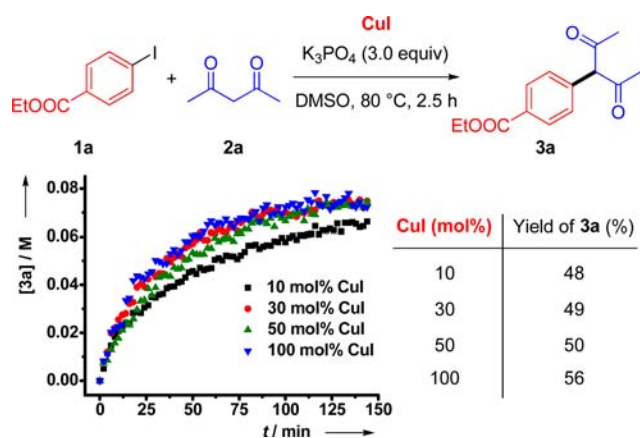


**Figure 1.** Kinetic profiles by employing different amounts of copper catalyst loadings. Reactions were monitored by operando IR. The yields of **3a** were determined by gas chromatography with naphthalene as the internal standard.

reaction provided the C–C cross-coupling product **3a** in 48% yield. To improve the reaction yields, we initially tried to employ higher catalyst loading. The reaction using 30 mol % CuI gave 49% yield, and the reaction of 50 mol % CuI afforded 50% yield. When even 100 mol % CuI was employed, the reaction yield was only 56%, which is quite strange and unanticipated. No obvious improvement has been achieved when more copper catalyst is employed. To gain more detailed information about this C–C bond forming reaction, kinetic experiments monitored by operando IR were carried out. As shown in Figure 1, it is interesting that the reactions not only have similar yields but also behave with similar kinetic features. The rate of this transformation was not accelerated by increasing the CuI catalyst. These results indicate that most of the CuI, which was added as the catalyst, is a spectator. An unknown copper species, which originated from CuI in the reaction solution, is the catalytically active species, and its concentration would not vary significantly with increasing the amount of CuI.

**Stepwise Stoichiometric Reaction between Acetylacetone **2a**, K<sub>3</sub>PO<sub>4</sub>, and CuI.** To elucidate the nature of the copper catalyst in this C–C bond forming reaction, the stepwise stoichiometric reactions between acetylacetone **2a**, K<sub>3</sub>PO<sub>4</sub>, and CuI were monitored by using operando IR.<sup>8</sup> The reaction vessel was first charged with **2a** in DMSO, followed by sequential addition of K<sub>3</sub>PO<sub>4</sub> and CuI. As shown in Figure 2a, after the addition of K<sub>3</sub>PO<sub>4</sub>, the broad peak of **2a** was

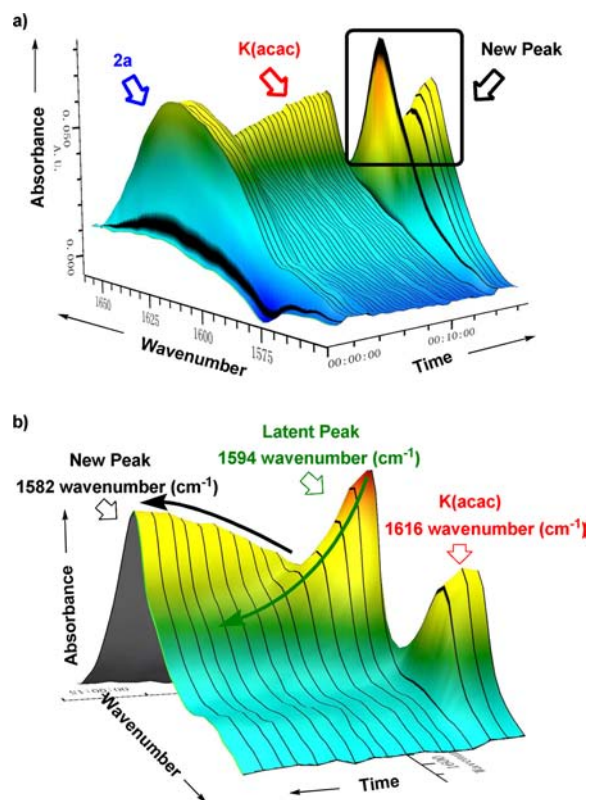


**Figure 2.** (a) Overall three-dimensional Fourier transform IR (3D-FTIR) profile of the stepwise stoichiometric reaction. (b) Amplification of the 3D-FTIR profile.

consumed, and a peak of K(acac) was accumulated. Then, addition of a stoichiometric amount of CuI to the mixture resulted in the consumption of K(acac) immediately and the formation of a new peak. At first glance, we deduced this new peak as the [Cu<sup>+</sup>(acac)L<sub>n</sub>] complex. However, the shape of the new peak was unusual (black frame in Figure 2a). Meanwhile, its ConCIRT spectrum<sup>9</sup> even looks like the spectrum of Cu(II)(acac)<sub>2</sub>.

After careful reinvestigation of this new peak, we found that its ConCIRT spectrum was broader in the 1606–1552 cm<sup>-1</sup> region than the authentic Cu(II)(acac)<sub>2</sub>. Amplification of this area disclosed very important information. As shown in Figure 2b, the peak of K(acac) at 1616 cm<sup>-1</sup> was fully consumed within 10 s after the addition of CuI. Meanwhile, a peak at 1594 cm<sup>-1</sup> was immediately accumulated to its maximum value also within 10 s. It is noteworthy that the peak at 1594 cm<sup>-1</sup> was then decreasing rapidly, and another new peak at 1582 cm<sup>-1</sup> was formed. In addition, we also clearly observed the formation of precipitate in the reaction vessel that is speculated as Cu metal.

Further data analysis with the iC IR software revealed more clear kinetic information, and the results are shown in Figure 3. The kinetic profiles of ConCIRT represent the concentration versus time, and the “component” represents a single compound. Three components were produced and detected from the stoichiometric reaction between **2a**, K<sub>3</sub>PO<sub>4</sub>, and CuI. Component I immediately decreased as soon as the addition of CuI. We could assign component I as the K(acac) complex I (1616 and 1511 cm<sup>-1</sup>, see the Supporting Information, Figure S1, also confirmed by <sup>13</sup>C NMR, Supporting Information, Figure S9). During the consumption of K(acac)(component I),

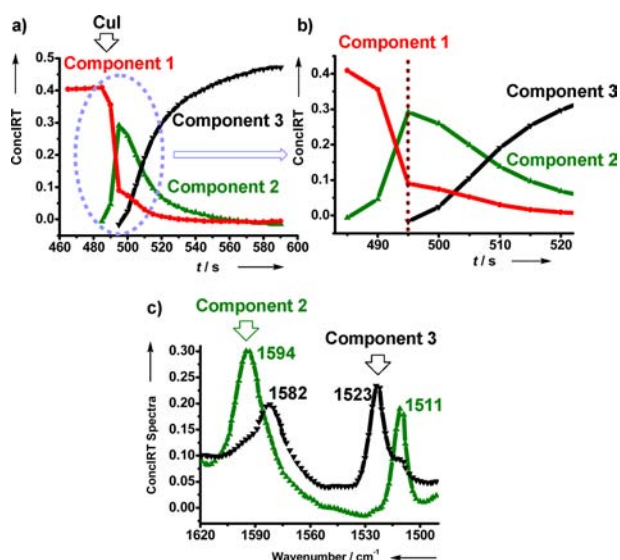
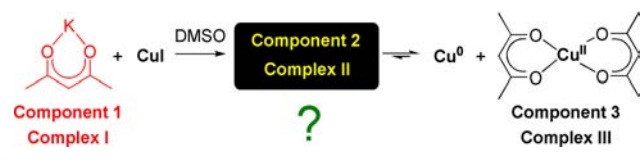


**Figure 3.** (a) Kinetic profiles of the stoichiometric reaction between K(acac) and CuI. (b) Amplification of IR profile. (c) The ConcIRT spectra of components 2 and 3.

one could observe the rapid formation of component 2. It is interesting to note that component 2 seemed to be an intermediate, which decreased readily. Meanwhile, a new component, 3, was formed simultaneously (Figure 3a). By comparing the ConcIRT spectrum with the authentic sample, component 3 was assigned to be Cu(II)(acac)<sub>2</sub> complex III (Figure 3c, 1582 and 1523 cm<sup>-1</sup>, see the Supporting Information, Figure S4).

As shown in Figure 3b, when CuI was introduced, the consumption of component 1 only generated component 2. However, without further addition of reactants, the consumption of component 2 could occur, and it generated component 3, which we preliminary assigned as Cu(II)(acac)<sub>2</sub> and some Cu-metal-like precipitate. That is to say, the compound represented by component 2 could disproportionate to Cu(0) and Cu(II)(acac)<sub>2</sub>.<sup>10</sup> Thus, it is reasonable to figure out that component 2 might be the [Cu<sup>+</sup>(acac)L<sub>n</sub>] complex II (Figure 3c, 1594 and 1511 cm<sup>-1</sup>). In a word, Cu(I) complex II, which rapidly formed from the reaction of K(acac) and CuI, was labile (Scheme 2).

#### Scheme 2. Stoichiometric Reaction between K(acac) and CuI



Furthermore, in situ X-ray absorption experiments were carried out toward the resulted solution and precipitate of the reaction of acetylacetone **2a** and K<sub>3</sub>PO<sub>4</sub> with CuI in DMF. As shown in Figure 4a, the Cu K-edge XANES spectrum of the reaction solution (line 1) with an edge energy of 8983.7 eV confirms the generation of Cu(II) species. Meanwhile, the edge energy (8979.0 eV) and features of the reaction precipitate (line 3) was characteristic of metallic Cu (line 4). The XANES provides direct evidence that the reaction of **2a** and K<sub>3</sub>PO<sub>4</sub> with CuI resulted in the formation of Cu(acac)<sub>2</sub> and metallic Cu.

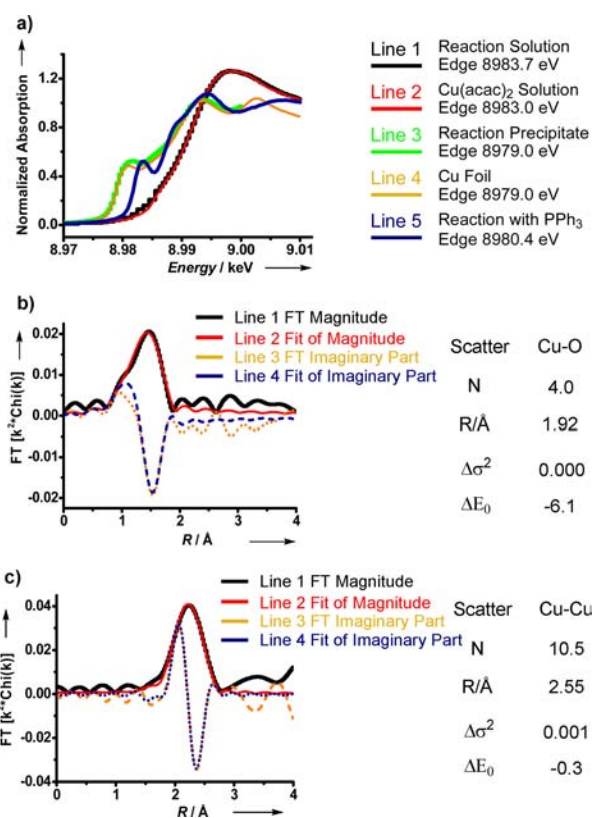


**Figure 4.** (a) Normalized Cu XANES spectra. Line 1: the solution of the reaction of **2a** and K<sub>3</sub>PO<sub>4</sub> with CuI. Line 2: the solution of authentic Cu(acac)<sub>2</sub>. Line 3: the precipitate of the reaction of **2a** and K<sub>3</sub>PO<sub>4</sub> with CuI. Line 4: Cu foil. Line 5: the solution of the reaction of **2a**, K<sub>3</sub>PO<sub>4</sub>, and CuI with PPh<sub>3</sub>. (b) k<sup>2</sup>-weighted R-space EXAFS spectra of the solution of the reaction of **2a** and K<sub>3</sub>PO<sub>4</sub> with CuI (2.8 < k < 10.8 Å<sup>-1</sup> and 0.9 < R < 1.8 Å). (c) k<sup>2</sup>-weighted R-space EXAFS spectra of the precipitate of the reaction of **2a** and K<sub>3</sub>PO<sub>4</sub> with CuI (2.7 < k < 12.1 Å<sup>-1</sup> and 1.6 < R < 2.7 Å).

In addition, the EXAFS data were also collected for the same reaction. The k<sup>2</sup>-weighted R-space spectra and a fit of the reaction solution are shown in Figure 4b. In the reaction solution, the Cu species was observed as four-oxygen bonded at a distance of 1.92 Å, which is identical to that of the DMF solution of Cu(acac)<sub>2</sub>. Meanwhile, the k<sup>2</sup>-weighted R-space spectra of the reaction precipitate and the fit are shown in Figure 4c. From the first shell fits, a Cu–Cu bond distance of 2.55 Å was determined. The coordination number of 10.5 indicates that the average particle size is about 6–7 nm.<sup>11</sup> The EXAFS also provides direct evidence that the reaction of **2a** and K<sub>3</sub>PO<sub>4</sub> with CuI resulted in the formation of Cu(acac)<sub>2</sub> and metallic Cu.

Complex II, which is speculated as [Cu<sup>+</sup>(acac)L<sub>n</sub>], is labile, and it is difficult to directly elucidate its structure even under mild conditions. The employment of extra ligand in the reaction might affect the disproportionation of the labile complex II and provide some structural information. Thus, further experiment using PPh<sub>3</sub> as the extra ligand was carried out. As shown in Figure 5a, when PPh<sub>3</sub> and CuI were introduced, complex I K(acac) (component A) was consumed rapidly, while a new component B was generated. Component B has nearly the same ConcIRT spectrum with complex II [Cu<sup>+</sup>(acac)L<sub>n</sub>] in the region 1500–1620 cm<sup>-1</sup> (see the Supporting Information, Figure S6) and was assigned as

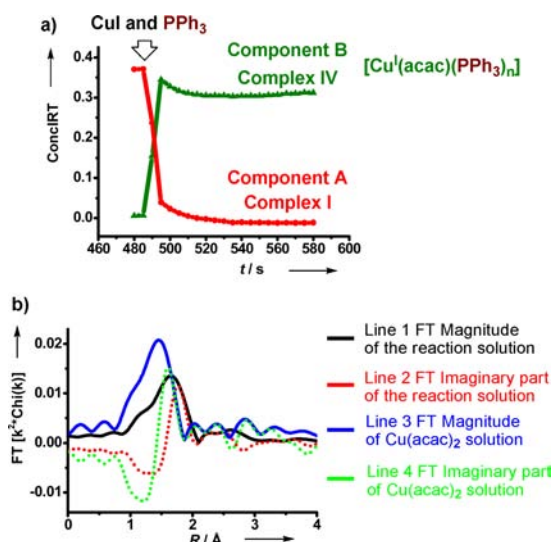


**Figure 5.** (a) Kinetic profiles of the reaction between **2a**,  $K_3PO_4$ , CuI, and  $PPh_3$ . Reaction was monitored by operando IR. (b)  $k^2$ -weighted  $R$ -space EXAFS spectra of  $Cu(acac)_2$  ( $2.8 < k < 10.8$ ) and the reaction of **2a**,  $K_3PO_4$ , and CuI with  $PPh_3$  ( $2.5 < k < 11.2$ ).

complex IV  $[Cu(I)(acac)(PPh_3)_n]$ . Kinetic profiles revealed that **complex IV** did not turn to  $Cu(II)(acac)_2$  as quick as **complex II** under the same conditions (Figure 5a). These results provided further evidence that we had directly observed the labile  $[Cu^+(acac)L_n]$  species by using operando IR, and the IR absorbances at  $1594$  and  $1511\text{ cm}^{-1}$  were its parts of the IR spectroscopic spectrum.

Moreover, the reaction of **2a**,  $K_3PO_4$ , and CuI in the presence of  $PPh_3$  was also investigated by the hard X-ray absorption experiment. As shown in Figure 4a, the edge energy of the solution with  $PPh_3$  (line 5) is shifted to  $8980.4\text{ eV}$  and has a pre-edge feature that is common for  $Cu^+$  compounds. In addition, it is clearly different from the reaction solution without  $PPh_3$  that is identical to that of  $Cu(acac)_2$  (Figure 5b). The magnitude peak for the solution with  $PPh_3$  is shifted to a longer distance, which is consistent with both Cu–O and Cu–P scatters. The Cu–P bond distance is longer than that of Cu–O. In addition, the different bond distance, phase, and amplitude result in interference of the two scatters leading to smaller peaks. The fits indicate there are two Cu–O bonds at  $2.03\text{ \AA}$ , that is, longer than that in  $Cu(acac)_2$  and two Cu–P bonds at  $2.21\text{ \AA}$  in the Cu coordination sphere. In addition, there is clearly no Cu–I bonds in the solution complex. In the presence of  $PPh_3$ , Cu does not disproportionate due to the  $PPh_3$  coordination. The in situ XANES/EXAFS experiments revealed that the structure of CuI with **2a**,  $K_3PO_4$ , and  $PPh_3$  in DMF is  $Cu(acac)(PPh_3)_2$ .

If this short-life  $[Cu^+(acac)L_n]$  species is the active catalyst in the C–C coupling reaction, the facile disproportionation will definitely cut down the reaction efficiency. Because  $PPh_3$  can increase the stability of the labile  $[Cu^+(acac)L_n]$  complex **II**, it may be beneficial for the catalytic C–C coupling reaction. Unfortunately, the yields were even lower by employing  $PPh_3$  in the reaction. This result indicated that increasing the stability of the intermediate catalyst would also decrease the reactivity in the catalytic reaction. Actually, some other common ligands were tested in the reactions. However, almost all those ligands suppressed the reaction more or less (see the Supporting Information, Table S1).

To further assess the potential structure of the complex **II**  $[Cu^+(acac)L_n]$  species, we computed the relative free energy of several possible forms of Cu(I) and Cu(II) species in the reaction solution (see the Supporting Information, Schemes S1 and S2). The tetrahedral-structured ate complex containing two acetylacetonate molecules most probably exists in the reaction. The density functional theory (DFT)-calculated IR absorbances of  $[Cu(I)(acac)_2]^-$  and  $Cu(II)(acac)_2$  were nicely in accordance with the experimental results in Figure 3c (Figure 6). The peaks in the  $1620\text{--}1550\text{ cm}^{-1}$  region were the  $\nu(C=$

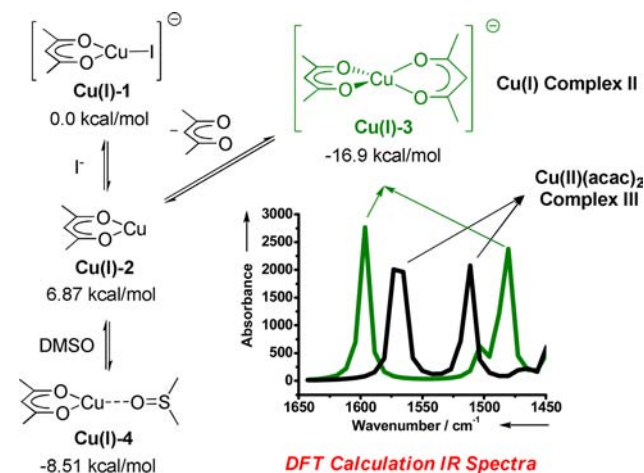


**Figure 6.** DFT calculation of the potential structure of complex **II**  $[Cu^+(acac)L_n]$  species and the IR absorbances of Cu(I) complex **II** and Cu(II) complex **III**.

O) stretching modes for the two copper  $\beta$ -diketonate complexes, while the peaks in the  $1530\text{--}1460\text{ cm}^{-1}$  region were the  $\nu(C=C)$  stretching modes.

**Stoichiometric Reactions Involving Aryl Iodide 1a.** To gain further insight of the Cu-catalyzed C–C coupling reaction, the reaction of **2a** ( $1.0\text{ mmol}$ ),  $K_3PO_4$  ( $1.5\text{ mmol}$ ), CuI ( $0.5\text{ mmol}$ ), and ethyl 4-iodobenzoate **1a** ( $0.5\text{ mmol}$ ) was investigated using operando IR. The kinetic profiles were compiled in Figure 7. The generation of the arylation product

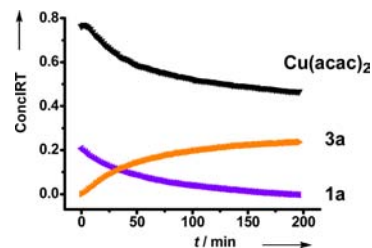
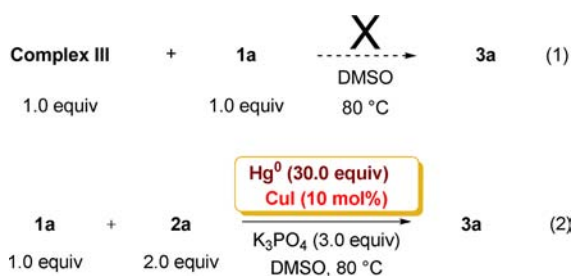


**Figure 7.** Kinetic profiles of the reaction of **2a**,  $K_3PO_4$ , CuI, and **1a**.

**3a** (orange curve) paralleled the consumption of **1a** (violet curve) (see the Supporting Information, Figures S7 and S8) and  $Cu(II)(acac)_2$ . This again indicated that, even under this condition, the formation of  $Cu(II)(acac)_2$  was facile. However, the direct stoichiometric reaction between  $Cu(II)(acac)_2$  and **1a** had also been examined (eq 1); no product **3a** was observed under the standard conditions.

From Figure 7, the mixture of **2a**,  $K_3PO_4$ , CuI, and **1a** would immediately generate  $Cu(II)(acac)_2$ , and no  $[Cu(I)(acac)_2]^-$  complex **II** is observed in the IR spectrum. The slow reaction,

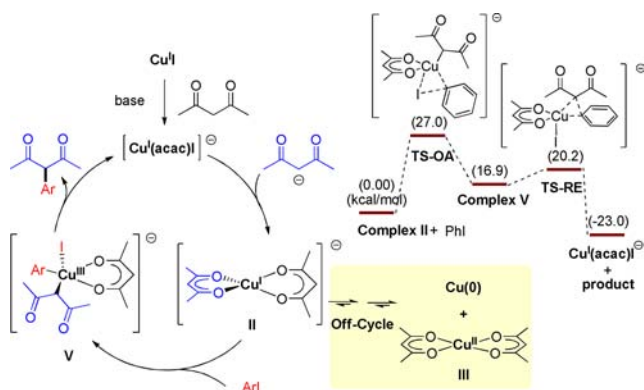


which led to the C–C coupling product **3a**, was different from eq 1. All these results indicated that the real catalytic species in the reaction of **2a**,  $\text{K}_3\text{PO}_4$ , CuI, and **1a** was only a trace amount, although 10, 30, 50, or even 100 mol % of the catalyst precursor was added.

To elucidate whether Cu(0) is the active catalyst for the transformation, a Hg(0)-poisoning experiment by adding excess Hg(0) was carried out. Generally, Hg(0) strongly poisons metal(0) catalysts by amalgamating the metal or adsorbing on its surface, which would obviously suppress the catalytic reaction.<sup>12</sup> As shown in (eq 2), 30 equiv of Hg(0) (300 equiv vs Cu catalyst) had no effect on the reaction. These experiments suggest that Cu(0) might not be the active catalyst.

**Discussion and Proposed Mechanism.** The investigations of these stoichiometric reactions inspired us to rationalize the “abnormal” reaction yields of different CuI loading and the kinetic observation in Figure 1. Although different amounts of CuI were employed, only the minority Cu(I) complex **II** might play a role as the actor catalyst. It is possible that there is an off-cycle process in this copper-catalyzed reaction (Scheme 3) that, no matter how much copper was used, the reaction rate and yield would not vary too much (Figure 1).

Scheme 3. Putative Mechanism of the Catalytic Cycle<sup>a</sup>



<sup>a</sup>TS-OA = transition state of oxidative addition. TS-RE = transition state of reductive elimination.

To assess the proposed reaction pathway for the activation of aryl iodide, we also computed the energy barrier for oxidative addition of ArI to Cu(I) complex **II**. The free energy of activation for oxidative addition of ArI to the Cu(I) complex to form the Cu(III) intermediate was calculated to be 27.9 kcal mol<sup>-1</sup> (see the Supporting Information, Figure S10). This computational result indicated that the Cu(III) species lie at energy that is accessible under this conditions.<sup>6</sup> Accordingly, the putative mechanism was shown in Scheme 3. The reaction was initiated by nucleophilic substitution to form labile Cu(I) complex **II**, which would easily disproportionate to the off-cycle

Cu(0) and Cu(II) species. Then, ArX could oxidatively add to Cu(I) complex **II** to generate a Cu(III) intermediate **V**. The resulting species underwent reductive elimination that would finally produce the corresponding product. Interestingly, in this copper-catalyzed transformation, acetylacetonate acted both as the substrate and the ligand.

## CONCLUSION

In conclusion, (1) we have directly observed and evidenced the labile complex of Cu(I) and a C nucleophile by operando IR and in situ XANES/EXAFS. (2) Kinetic studies and computational calculations revealed that this labile  $\beta$ -diketone Cu(I) species might be the active catalyst for the copper-catalyzed C–C coupling reaction. The labile Cu(I) species could rapidly disproportionate to the spectator Cu(II) and Cu(0) species in the reaction, which was an off-cycle process. (3)  $\text{PPh}_3$  could stabilize the labile Cu(I)  $\beta$ -diketonate species. However, it also inhibited the reactivity of the C–C coupling reaction. (4) In this copper-catalyzed arylation,  $\beta$ -diketone might act both as the substrate and the ligand. We believe that these kinetic investigations provide a useful insight into the nature of catalytic reaction, which will be helpful for the understanding of the mechanism and for the synthetic applications.

## ASSOCIATED CONTENT

### Supporting Information

General information, experimental details and characterization, and computational calculation details. This material is available free of charge via the Internet at <http://pubs.acs.org>.

## AUTHOR INFORMATION

### Corresponding Author

aiwenlei@whu.edu.cn

### Notes

The authors declare no competing financial interest.

## ACKNOWLEDGMENTS

This work was supported by the “973” Project from the MOST of China (2011CB808600) and the National Natural Science Foundation of China (21025206, 20832003, 20972118, 20972119). The authors also thank the support from “the Fundamental Research Funds for the Central Universities”, Program for New Century Excellent Talents in University (NCET) and Program for Changjiang Scholars and Innovative Research Team in University (IRT1030). Use of the Advanced Photon Source was supported by the U.S. Department of Energy, Office of Basic Energy Sciences, under contract no. DE-AC02-06CH11357. MRCAT operations are supported by the Department of Energy and the MRCAT member institutions. Partial funding for J.T.M. was provided by Chemical Sciences, Geosciences and Biosciences Division, U.S. Department of Energy, under contract no. DE-AC02-06CH11357. This work was also funded by the Chemical Sciences and Engineering Division at Argonne National Laboratory. In addition, we thank Prof. Mei-Xiang Wang (Tsinghua University) for providing Cu(III) sample as gift.

## REFERENCES

- (1) (a) Krause, N. *Modern Organocopper Chemistry*; Wiley-VCH: Weinheim, Germany, 2002; (b) Ley, S. V.; Thomas, A. W. *Angew. Chem., Int. Ed.* **2003**, *42*, 5400–5449. (c) Monnier, F.; Taillefer, M. *Angew. Chem., Int. Ed.* **2009**, *48*, 6954–6971. (d) Hassan, J.; Sevignon,

M.; Gozzi, C.; Schulz, E.; Lemaire, M. *Chem. Rev.* **2002**, *102*, 1359–1469. (e) Chemler, S. R.; Fuller, P. H. *Chem. Soc. Rev.* **2007**, *36*, 1153–1160. (f) Beletskaya, I. P.; Cheprakov, A. V. *Coord. Chem. Rev.* **2004**, *248*, 2337–2364. (g) Finet, J.-P.; Fedorov, A. Y.; Combes, S.; Boyer, G. *Curr. Org. Chem.* **2002**, *6*, 597–626. (h) Sperotto, E.; van Klink, G. P. M.; van Koten, G.; de Vries, J. G. *Dalton Trans.* **2010**, *39*, 10338–10351. (i) Evano, G.; Blanchard, N.; Toumi, M. *Chem. Rev.* **2008**, *108*, 3054–3131.

(2) Paine, A. J. *J. Am. Chem. Soc.* **1987**, *109*, 1496–1502.

(3) (a) Weingarten, H. *J. Org. Chem.* **1964**, *29*, 3624–3626. (b) Aalten, H. L.; Van Koten, G.; Grove, D. M.; Kuilman, T.; Piekstra, O. G.; Hulshof, L. A.; Sheldon, R. A. *Tetrahedron* **1989**, *45*, 5565–5578. (c) Jones, G. O.; Liu, P.; Houk, K. N.; Buchwald, S. L. *J. Am. Chem. Soc.* **2010**, *132*, 6205–6213. (d) Strieter, E. R.; Bhayana, B.; Buchwald, S. L. *J. Am. Chem. Soc.* **2009**, *131*, 78–88. (e) Strieter, E. R.; Blackmond, D. G.; Buchwald, S. L. *J. Am. Chem. Soc.* **2005**, *127*, 4120–4121. (f) Tye, J. W.; Weng, Z.; Giri, R.; Hartwig, J. F. *Angew. Chem., Int. Ed.* **2010**, *49*, 2185–2189. (g) Tye, J. W.; Weng, Z.; Johns, A. M.; Incarvito, C. D.; Hartwig, J. F. *J. Am. Chem. Soc.* **2008**, *130*, 9971–9983. (h) Cristau, H.-J.; Cellier, P. P.; Spindler, J.-F.; Taillefer, M. *Chem.—Eur. J.* **2004**, *10*, 5607–5622. (i) Franc, G.; Cacciuto, Q.; Lefevre, G.; Adamo, C.; Ciofini, I.; Jutand, A. *ChemCatChem* **2011**, *3*, 305–309. (j) Franc, G.; Jutand, A. *Dalton Trans.* **2010**, *39*, 7873–7875. (k) Mansour, M.; Giacomazzi, R.; Ouali, A.; Taillefer, M.; Jutand, A. *Chem. Commun.* **2008**, 6051–6053. (l) Ouali, A.; Spindler, J.-F.; Jutand, A.; Taillefer, M. *Adv. Synth. Catal.* **2007**, *349*, 1906–1916. (m) Yu, H.-Z.; Jiang, Y.-Y.; Fu, Y.; Liu, L. *J. Am. Chem. Soc.* **2010**, *132*, 18078–18091. (n) Zhang, S.; Ding, Y. *Organometallics* **2011**, *30*, 633–641. (o) Zhang, S.-L.; Liu, L.; Fu, Y.; Guo, Q.-X. *Organometallics* **2007**, *26*, 4546–4554. (p) Savarin, C.; Srogl, J.; Liebeskind, L. S. *Org. Lett.* **2002**, *4*, 4309–4312. (q) Ma, D.; Zhang, Y.; Yao, J.; Wu, S.; Tao, F. *J. Am. Chem. Soc.* **1998**, *120*, 12459–12467. (r) Allred, G. D.; Liebeskind, L. S. *J. Am. Chem. Soc.* **1996**, *118*, 2748–2749. (s) Liu, S.; Yu, Y.; Liebeskind, L. S. *Org. Lett.* **2007**, *9*, 1947–1950. (t) Kaddouri, H.; Vicente, V.; Ouali, A.; Quazzani, F.; Taillefer, M. *Angew. Chem., Int. Ed.* **2009**, *48*, 333–336. (u) Jerphagnon, T.; van Link, G. P. M.; de Vries, J. G.; van Koten, G. *Org. Lett.* **2005**, *7*, 5241–5244.

(4) (a) Hurlley, W. R. H. *J. Chem. Soc.* **1929**, 1870–1873. (b) Bruggink, A.; Ray, S. J.; McKillop, A. *Org. Synth.* **1978**, *58*, 52–56. (c) Setsune, J.; Matsukawa, K.; Wakemoto, H.; Kitao, T. *Chem. Lett.* **1981**, 367–370. (d) Setsune, J.; Matsukawa, K.; Kitao, T. *Tetrahedron Lett.* **1982**, *23*, 663–666. (e) Setsune, J.; Ueda, T.; Shikata, K.; Matsukawa, K.; Iida, T.; Kitao, T. *Tetrahedron* **1986**, *42*, 2647–2656.

(5) (a) Hennessy, E. J.; Buchwald, S. L. *Org. Lett.* **2002**, *4*, 269–272. (b) Chen, Y.; Wang, Y.; Sun, Z.; Ma, D. *Org. Lett.* **2008**, *10*, 625–628. (c) Xie, X.; Cai, G.; Ma, D. *Org. Lett.* **2005**, *7*, 4693–4695. (d) Xie, X.; Chen, Y.; Ma, D. *J. Am. Chem. Soc.* **2006**, *128*, 16050–16051. (e) Yip, S. F.; Cheung, H. Y.; Zhou, Z.; Kwong, F. Y. *Org. Lett.* **2007**, *9*, 3469–3472. (f) Jiang, Y.; Wu, N.; Wu, H.; He, M. *Synlett* **2005**, 2731–2734. (g) He, C.; Guo, S.; Huang, L.; Lei, A. *J. Am. Chem. Soc.* **2010**, *132*, 8273–8275.

(6) Huang, Z.; Hartwig, J. F. *Angew. Chem., Int. Ed.* **2012**, *51*, 1028–1032.

(7) (a) Nelson, R. C.; Miller, J. T. *Catal. Sci. Technol.* **2012**, *2*, 461–470. (b) Bañares, M. A. *Catal. Today* **2005**, *100*, 71–77. (c) Ellis, P. J.; Fairlamb, I. J. S.; Hackett, S. F. J.; Wilson, K.; Lee, A. F. *Angew. Chem., Int. Ed.* **2010**, *49*, 1820–1824.

(8) Usually,  $\beta$ -diketone compounds were employed as ligands in copper-catalyzed reactions,<sup>31</sup> for which the nucleophilic substitution might occur first to form the complex of copper and nucleophile.

(9) Relative concentration profiles are calculated by ConcIRT LIVE for products, intermediates, and starting materials. ConcIRT LIVE is especially valuable for trending chemical species that have overlapping peaks. ConcIRT LIVE uses a type of mathematical algorithm known as curve-resolution. Curve-resolution algorithms have the capability to group wavenumber values that change absorbance intensity in the same manner. For each group, ConcIRT LIVE calculates the

associated component spectrum and relative concentration profile. As each new reaction spectrum is acquired, ConcIRT LIVE reanalyzes all the reaction spectra and updates the individual component spectra and profiles. Thus, the calculation results evolve as the reaction proceeds, and additional components such as intermediates are detected. ConcIRT LIVE Component Spectra: The correspondence between measured pure component spectra and the extracted spectra calculated by ConcIRT LIVE is usually more than sufficient to identify reaction species. Especially useful, ConcIRT LIVE frequently makes it possible to determine when transient intermediates are present.

(10) (a) Shin, H. K.; Hampden-Smith, M. J.; Duesler, E. N.; Kodas, T. T. *Can. J. Chem.* **1992**, *70*, 2954–2966. (b) Chen, T. Y.; Vaisermann, J.; Ruiz, E.; Senateur, J. P.; Doppelt, P. *Chem. Mater.* **2001**, *13*, 3993–4004. (c) Shin, H. K.; Chi, K. M.; Farkas, J.; Hampden-Smith, M. J.; Kodas, T. T.; Duesler, E. N. *Inorg. Chem.* **1992**, *31*, 424–431.

(11) Miller, J. T.; Kropf, A. J.; Zha, Y.; Regalbutto, J. R.; Delannoy, L.; Louis, C.; Bus, E.; Van Bokhoven, J. A. *J. Catal.* **2006**, *240*, 222–234.

(12) (a) Whitesides, G. M.; Hackett, M.; Brainard, R. L.; Lavalle, J. P. P. M.; Sowinski, A. F.; Izumi, A. N.; Moore, S. S.; Brown, D. W.; Staudt, E. M. *Organometallics* **1985**, *4*, 1819–1830. (b) Widegren, J. A.; Bennett, M. A.; Finke, R. G. *J. Am. Chem. Soc.* **2003**, *125*, 10301–10310.